ChemComm

Accepted Manuscript

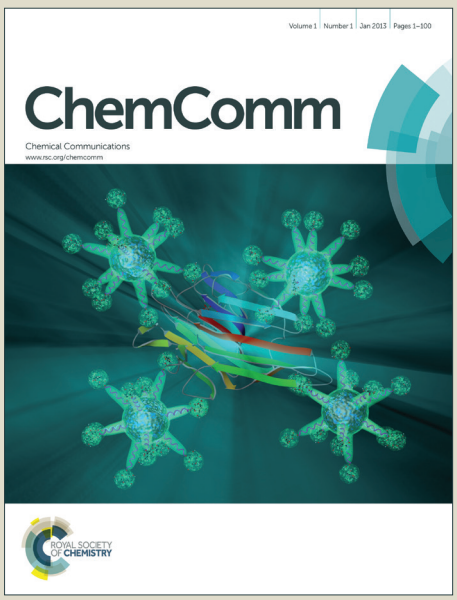

ROYAL SOCIETY OF CHEMISTRY

www.rsc.org/chemcomm

Journal Name

RSCPublishing

COMMUNICATION

A folate receptor-specific activatable probe for near-infrared fluorescence imaging of ovarian cancer

Cite this: DOI: 10.1039/x0xx00000x

Hawon Lee[a]‡, Jisu Kim[a]‡, Hyunjin Kim[a], Youngmi Kim[b] and Yongdoo Choi*[a]

Received 00th January 2012,
Accepted 00th January 2012

DOI: 10.1039/x0xx00000x

www.rsc.org/

We have developed a folate receptor-specific activatable probe for near-infrared fluorescence imaging of ovarian cancer *in vivo*. This probe becomes highly fluorescent only when its linker is cleaved by tumor-associated lysosomal enzyme cathepsin B after internalization into folate receptor-positive cancer cells.

Ovarian cancer, the leading cause of cancer-related death in women in the United States,[1] is often called the "silent lady killer" because there are no disease-specific symptoms until the disease has progressed to an advanced stage.[2] Moreover, there is a lack of a specific screening methods available for early diagnosis. Although simultaneous screening with CA-125 (a serum tumor marker) and transvaginal ultrasound can detect ovarian cancer, these methods do not reduce ovarian cancer mortality because of high rate of false positivity.[2,3] As a result, 75% of patients are diagnosed with the disease at the advanced stage, with wide-spread peritoneal carcinomatosis, and the 5-year survival rates for stage Ⅳ cancer are only about 30%.[1] Currently, residual tumor size after cytoreductive surgery is one of the most important prognostic factors in advanced ovarian cancer,[4] with sizes of either >1 cm, ≤1 cm, or microscopic sizes being closely related with the survival outcome.

Fluorescence imaging technology is a useful tool for real-time *in vivo* imaging with high sensitivity and resolution.[5] Since 90–95% of ovarian cancers overexpress folate receptor-α (FAR), this receptor is considered a good target for ovarian cancer imaging,[6] and various types of folate-fluorochrome conjugates has been developed for tumor-specific image-guided surgery.[7] Most recently, van Dam et al. performed the first clinical trial of image-guided cytoreduction of peritoneally seeded ovarian tumors after intravenous administration of folate-conjugated fluorescein isothiocyante.[8] According to this report, this fluorescence image-guided technique not only improved the detection rate of ovarian tumors in the peritoneal region (four-fold higher than that by visual observation alone), but could also detect masses of a smaller size.

Since most of the currently developed folate-fluorochrome conjugates are "always-on" type agents, high background fluorescence signals of these conjugates results in a low target-to-background ratio when circulating in the blood stream. Therefore, the development of near-infrared (NIR) fluorescence imaging agent with not only target-cell specificity, but also a high tumor-to-background ratio is required, but has been highly challenging.

Here we synthesized a folate receptor-specific activatable (FSA) probe for *in vivo* fluorescence imaging of ovarian cancer (Figure 1A and B). In contrast with "always on" type agents, the FSA probe is expected to show an enhanced performance by maximizing the target signals while minimizing the background signals, thereby enabling the obtainment of a high target-to-background ratio.

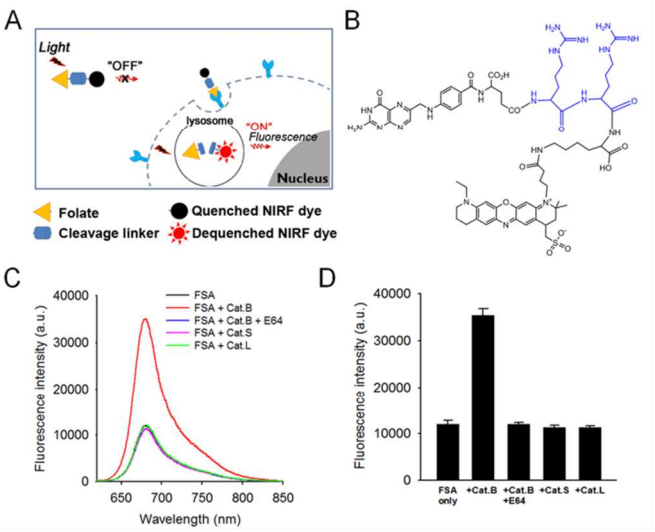

Fig. 1 (a) Schematic diagram of the folate receptor-specific fluorescence activation of the FSA probe in ovarian cancer cells. (b) The structure of the FSA probe. Folate and ATTO655 are connected by di-arginines (RR). (c) Representative fluorescence spectra of the FSA probe and probes treated with cathepsin B (Cat. B), E64-pretreated cathepsin B, cathepsin S (Cat. S), and cathepsin L (Cat. L) ($\lambda_{ex.}$ 610 nm). (d) Changes in fluorescence intensity ($\lambda_{ex.}$ 610 nm, $\lambda_{em.}$ 680 nm) of the FSA probe under various conditions (n = 3).

Until now, folate (FA) has been solely used to target FAR, which is expressed on the cancer cell surface.[9] However, in this study, FA is used not only as a targeting moiety for FAR, but also as a quencher for the NIR fluorescence dye. The FSA probe was synthesized by conjugating the ATTO655 dye to FA *via* a short

peptide linker. We hypothesized that the fluorescence emission by ATTO655 dye may be effectively controlled by the distance between the FA and the dye. In its conjugated state, the NIR dye ATTO655 is in close proximity to FA, and fluorescence emission from the dye is effectively quenched (OFF). When FSA probes specifically bind to FAR on the surface of ovarian cancer cells and become internalized *via* receptor-mediated endocytosis, cleavage of the peptide linkers by the tumor-associated lysosomal enzyme (cathepsin B)[10] occurs, resulting in the release of the NIR dye from the FSA probe and subsequent activation of fluorescence emission (ON) of the dye.

The molecular weight of the purified FSA conjugate was 1,391 g/mol (Fig. S1 and S2). Absorption and emission peaks of FSA were 665 nm and 680 nm, respectively (Fig. S3 and Fig. 1C).

Figs. 1C and D show the activation of fluorescence emission upon cathepsin B treatment. A 3-fold increase in fluorescence intensity was observed for FSA treated with cathepsin B, compared to the buffer-treated FSA probe. Pretreatment of cathepsin B with its inhibitor (E64) completely inhibited the increase in the FSA fluorescence. Treatment of the FSA probe with other cathepsins (i.e., cathepsin S and L which are lysosomal enzymes with similar arginine selectivity)[10d] did not induce an increase in fluorescence intensity, which confirmed that this effect is specific to cathepsin B. Owing to the absence of overlap between the fluorescence emission of ATTO655 and the absorbance of FA, fluorescence resonance energy transfer from ATTO655 to FA should be excluded. One potential mechanism of quenching might be photoinduced electron transfer (PET).[11]

We then checked if presence of serum proteins could induce nonspecific activation of FSA fluorescence (Fig. S4). The FSA probes (1 μM) were dissolved in phosphate-buffered saline (PBS, 6.7 mM, pH 7.4, 154 mM NaCl), PBS containing 20% human serum albumin (HSA), or 100% fetal bovine serum (FBS). After incubation for 4 h, no increase in the fluorescence intensity of FSA was observed in either the presence of HSA or FBS, confirming that serum proteins do not affect the fluorescence turn-on of the FSA probe.

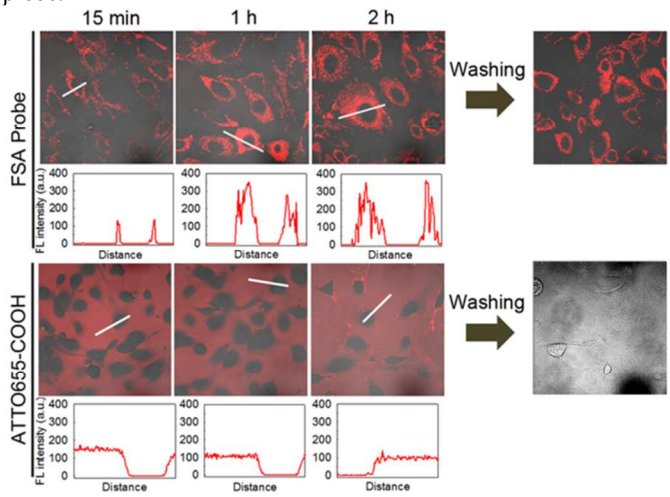

Fig. 2 Fluorescence quenching and activation of FSA within target cells (left-hand side panels). Confocal microscopy images (upper row) of SKOV3 cells obtained using a confocal laser scanning microscope ($\lambda_{ex.}$ 633 nm, $\lambda_{em.}$ 646~753 nm). SKOV3 cells were incubated with 1 μM FSA probe solution or ATTO655, and fluorescence images were obtained without washing the cells at 15 min, 1 h, and 2 h. The fluorescence intensity across the area indicated by the white lines in the upper row was analyzed. Additional images (right-hand side panel) were obtained after washing the cells 2 h post-incubation to rule out the nonspecific uptake of free dyes.

Next, the utility of FSA probe in activatable NIR fluorescence imaging of ovarian cancer cells was tested in *in vitro* cell studies. Both the FSA probe and a free dye (ATTO655) were applied to FAR-overexpressing SKOV3 cells at a concentration of 1 μM. Because the NIR fluorescence signals from the FSA probe were expected to be turned-off in the extracelluar space and activated only inside the target cancer cells, we obtained NIR fluorescence images ($\lambda_{ex.}$ 633 nm, $\lambda_{em.}$ 646~753 nm) of the cells without washing them at 15 min, 1 h, and 2 h using a confocal laser scanning microscope (Fig. 2). As expected, weak fluorescence signals were detected in the extracelluar space of the FSA-treated cells for 2 h, whereas strong fluorescence signals were observed in the free dye-treated cancer cells. Fluorescence intensities generated inside the FSA-treated cells become stronger with time, indicating activation of fluorescence emission in the target cells with time. When the cells were washed after 2 h and NIR fluorescence images was acquired again, no fluorescence signals was observed in the free dye-treated cells, confirming that hydrophilic free dyes did not enter SKOV3 cells in a nonspecific manner. In the FSA-treated cells, strong fluorescence signals were still shown inside the cells even after washing procedure (Fig. 2, upper right). These data confirm that FSA probe is useful in NIR fluorescence imaging of the target cancer cells with a high target-to-background ratio.

Then we checked if the turn-on of the FSA probe fluorescence inside SKOV3 cells (Fig. 3) was due to folate receptor-mediated endocytosis and subsequent activation of fluorescence emission by cathepsin B activity. As shown in Fig. 3, folate receptor-positive SKOV3 cells showed strong fluorescence upon treatment of FSA probe whereas folate receptor-negative A549 cells showed little to no fluorescence. When the SKOV3 cells were treated with the FSA probe in the presence of excess free FA as a competitor, the cells become weakly fluorescent. In addition, pretreatment of SKOV3 cells with the cell-permeable cathepsin B inhibitor (E64d) resulted in significant reduction of fluorescence within the cells, indicating that the fluorescence of the internalized FSA probes could be turned-on by this protease. These results confirm that FSA probe was internalized within the cells *via* FAR-mediated endocytosis, and then its fluorescence was activated by the lysosomal cathepsin B activity.

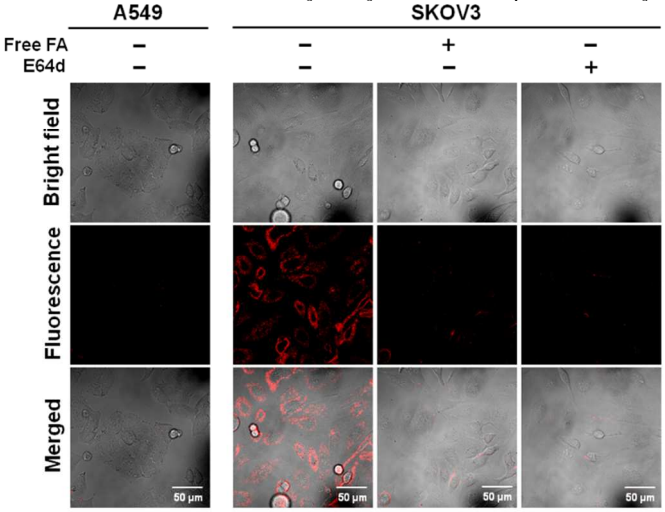

Fig. 3 Receptor-mediated intracellular uptake and subsequent fluorescence activation of FSA. Confocal microscopy images of FAR-negative A549 and FAR-positive SKOV3 cells were obtained after 2 h of FSA treatment ($\lambda_{ex.}$ 633 nm, $\lambda_{em.}$ 646~753 nm). For competition assay, free FA (1 mM) was co-incubated with FSA. For enzyme inhibition test, SKOV3 cells were pretreated with E64d (cell-permeable cathepsin B inhibitor, 20 μM), and then incubated with FSA.

Finally, we used a xenografted mouse model to assess the utility of the FSA probe for *in vivo* fluorescence imaging of FAR-positive ovarian cancer tissues. All the mice received a subcutaneous

injection of the SKOV3 cancer cells in the hind flank, and tumors were allowed to grow to ~60 mm^3. The mice in the free dye (ATTO655)-treated and FSA-treated groups received intravenous injections of the dyes at the dose of 15 nmol/20 g body weight, while those in the control group received PBS intravenously (100 μL/mouse). NIR fluorescence images ($\lambda_{ex.}$ 660 nm, $\lambda_{em.}$ 690~730 nm) were obtained 3 h post-injection. As shown in Fig. 4A, strong fluorescence signals were observed in tumors of the FSA-treated mice, with a high tumor-to-background ratio of 7.76 ± 0.88. Since most of the hydrophilic free dyes were rapidly eliminated *via* urinary excretion within 30 min of injection (data not shown), no accumulation of the free dye was observed at the tumor sites. As a result, no difference in fluorescence intensities between tumor tissue and surrounding background was observed in the PBS- and free dye-treated mice at 3 h post-injection. *Ex vivo* fluorescence images of organs also showed that the strong fluorescent signals in the FSA-treated mice came from the tumors (Figure 4C). These results indicate that the FSA probe selectively accumulates in the target tumor tissues, where its fluorescence is subsequently activated.

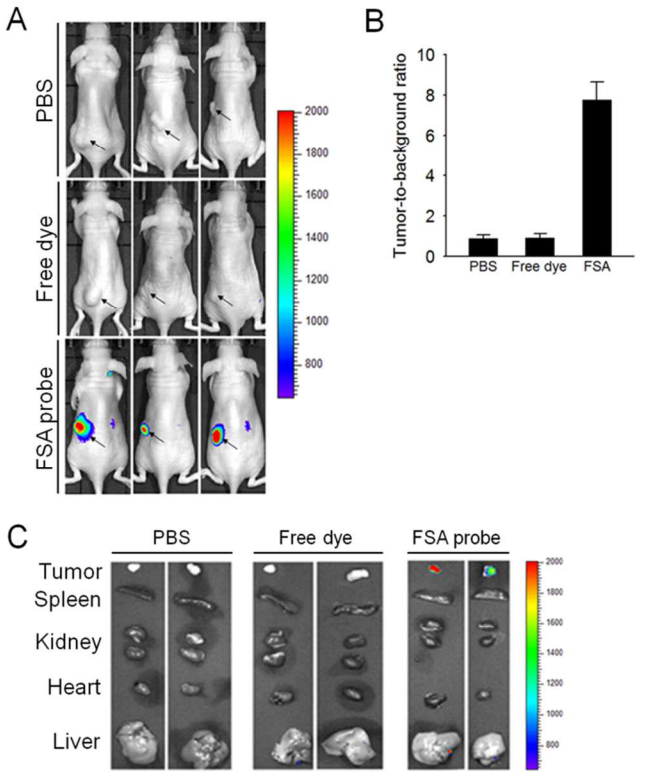

Fig. 4. (A) NIR fluorescence images of SKOV3 tumor-bearing mice ($\lambda_{ex.}$ 660 nm, $\lambda_{em.}$ 690~730 nm) that received intravenous injections of PBS, the free ATTO655 dye, or FSA. The images were obtained 3 h post-injection. Arrows indicate tumor sites. (B) Tumor-to-background ratios of the fluorescence intensities (n = 3). (C) Representative *ex vivo* fluorescence images of organs and tumors from the SKOV3 tumor-bearing mice 3 h after PBS, free dye, or FSA administration ($\lambda_{ex.}$ 660 nm, $\lambda_{em.}$ 690~730 nm).

Based on our previous study,[12] we expect that NIR fluorescence imaging can be used with an FSA probe to detect peritoneally seeded ovarian cancer cells located in deeper tissues (i.e., up to 9 mm depth).

Conclusions

An FSA probe was synthesized by conjugating FA with the ATTO655 dye *via* a cathepsin B-cleavable peptide linker. This probe showed FAR-specific uptake into SKOV3 cell, with subsequent activation of NIR fluorescence by the action of tumor-associated cathepsin B enzymes inside the cells. Utility of FSA in the FAR-specific activiatable fluorescence imaging was also evaluated using an *in vivo* xenograft model of ovarian cancer.

This work was supported by a National Cancer Center grant (1310160), Republic of Korea.

Notes and references

[a] Molecular Imaging & Therapy Branch, National Cancer Center, 323 Ilsan-ro, Goyang-si, Gyeonggi-do 410-769, Korea. E-mail: ydchoi@ncc.re.kr; Fax: +82-31-920-2529; Tel: +82-31-920-2512
[b] Department of Chemistry, Institute of Nanosensor and Biotechnology, Dankook University, 126 Jukjeon-dong, Yongin-si, Gyeonggi-do 448-701, Korea.
‡ Equally contributed to this work
† Electronic Supplementary Information (ESI) available: See DOI: 10.1039/c000000x/

1 R. Siegel, D. Naishadham, A. Jemal, *CA Cancer J. Clin.*, 2013, **63**, 11.
2 (a) S. S. Buys, E. Partridge, A. Black, C. C. Johnson, L. Lamerato, C. Isaacs, D. J. Reding, R. T. Greenlee, L. A. Yokochi, B. Kessel, E. D. Crawford, T. R. Church, G. L. Andriole, J. L. Weissfeld, M. N. Fouad, D. Chia, B. O'Brien, L. R. Ragard, J. D. Clapp, J. M. Rathmell, T. L. Riley, P. Hartge, P. F. Pinsky, C. S. Zhu, G. Izmirlian, B. S. Kramer, A. B. Miller, J.-L. Xu, P. C. Prorok, J. K. Gohagan, C. D. Berg, *JAMA*, 2011, **305**, 2295. (b) M.C. Lim, S.S. Seo, S. Kang, S.K. Kim, S.H. Kim, C.W. Yoo, S.Y. Park, *Quant. Imaging Med. Surg.*, 2012, **2**, 114.
3 P. A. Canney, M. Moore, P. M. Wilkinson, R. D. James, *Br. J. Cancer*, 1984, **50**, 765.
4 M. Polcher, O. Zivanovic, D. S. Chi, *Womens Health (Lond Engl)*, 2014, **10**, 179.
5 K. Gotoh, T. Yamada, O. Ishikawa, H. Takahashi, H. Eguchi, M. Yano, H. Ohigashi, Y. Tomita, Y. Miyamoto, S. Imaoka, *J. Surg. Oncol.*, 2009, **100**, 75.
6 (a) K. R. Kalli, A. L. Oberg, G. L. Keeney, T. J. Christianson, P. S. Low, K. L. Knutson, L. C. Hartmann, *Gynecol. Oncol.*, 2008, **108**, 619. (b) S. Markert, S. Lassmann, B. Gabriel, M. Klar, M. Werner, G. Gitsch, F. Kratz, A. Hasenburg, *Anticancer Res.* 2008, **28**, 3567.
7 (a) W. K. Moon, Y. Lin, T. O'Loughlin, Y. Tang, D. E. Kim, R. Weissleder, C. H. Tung, *Bioconjug. Chem.*, 2003, **14**, 539. (b) H. Meng, J. Y. Chen, L. Mi, P. N. Wang, M. Y. Ge, Y. Yue, N. Dai, *J. Biol. Inorg. Chem.*, 2011, **16**, 117. (c) J. Yang, H. Chen, I. R. Vlahov, J. X. Cheng, P. S. Low, *Proc. Natl. Acad. Sci. U.S.A* 2006, **103**, 13872. (d) J. Ai, Y. Xu, D. Li, Z. Liu, E. Wang, *Talanta* 2012, **101**, 32. (e) J. Qiao, X. Mu, L. Qi, J. Deng, L. Mao, *Chem. Commun*., 2013, **49**, 8030.
8 G. M. van Dam, G. Themelis, L. M. Crane, N. J. Harlaar, R. G. Pleijhuis, W. Kelder, A. Sarantopoulos, J. S. de Jong, H. J. Arts, A. G. van der Zee, J. Bart, P. S. Low, V. Ntziachristos, *Nat Med*, 2011, **17**, 1315.
9 P. S. Low, S. A. Kularatne, *Curr. Opin. Chem. Biol.*, 2009, **13**, 256.
10 (a) K. I. Hulkower, C. C. Butler, B. E. Linebaugh, J. L. Klaus, D. Keppler, V. L. Giranda, B. F. Sloane, *Eur. J. Biochem.*, 2000, **267**, 4165.

(b) A. J. Barrett, *Anal. Biochem.*, 1976, **76**, 374. (c) A. J. Barrett, *Biochem. J.*, 1980, **187**, 909. (d) A. J. Barrett, H. Kirschke, *Methods Enzymol.*, 1981, **80**, 535.

11 (a) Y. Zhang, J. M. Liu, X. P. Yan, *Anal. Chem*., 2013, **85**, 228. (b) S. E. Mansoor, M. A. Dewitt, D. L. Farrens, *Biochemistry*, 2010, **49**, 9722.

12 Y. Choi, K. G. Kim, J. K. Kim, K. W. Nam, H. H. Kim, D. K. Sohn, *Surg Endosc.*, 2011 , **25**, 2372.

